Synthesis, Crystal Structure, and Thermal Decomposition Kinetics of the Sm^{3+} Complex with *p*-Chlorobenzoic Acid and 2,2′-Bipyridine

Jian-Jun Zhang,*[,†,‡] Hai-Yan Zhang,[†,‡] Xue Zhou,[§] Ning Ren,[||] and Shu-Ping Wang[‡]

Experimental Center, Hebei Normal University, Shijiazhuang 050016, P. R. China, College of Chemistry & Material Science, Hebei Normal University, Shijiazhuang 050016, P. R. China, Shijiazhuang Economy College, Shijiazhuang 050031, P. R. China, and Department of Chemistry, Handan College, Handan 056005, P. R. China

A dinuclear samarium(III) complex $[Sm(p\text{-ClBA})_3bipy\cdot H_2O]_2$ [*p*-ClBA = *p*-chlorobenzoate; bipy = 2,2′-bipyridine] has been synthesized and characterized by elemental analysis, molar conductance, UV and IR spectra, and TG−DTG techniques. Single-crystal X-ray diffraction analysis revealed that each Sm^{3+} ion in the compound is eight-coordinated with the bicapped triangular prism geometry. The crystal belongs to the triclinic system, space group $P\bar{1}$. The thermal decomposition behavior of the title complex in a static air atmosphere was investigated by TG−DTG and IR techniques. Meanwhile, the nonthermal kinetics of the second decomposition stage was also studied by using a double equal−double steps method and the nonlinear integral isoconversional method.

Introduction

The complexes of rare earth (RE) and organic ligands with certain conjugated systems have been widely applied in micro rare earth analysis, photoluminescence material, and laser work matter due to their strong fluorescence properties.[1] The oxygen atoms of the carboxylic group can be bonded to RE(III) through various modes, namely, monodentate, bidentate-chelating, bidentate-bridging, bidentate-chelating−bridging, and so on. Therefore, there are plural special structures for rare earth carboxylic acid complexes, such as infinity-chain structures and net-layered polymerization structures.[2] Hence much attention has been paid to the relationship between structure and property. The crystal structures of a series of rare earth complexes with nitrogen-containing ligands and benzoic acid and its derivatives have been extensively studied.[3−7]

Thermal analysis dynamics is widely applied in research on phase transformation and chemical reaction processes, such as dehydration, decomposition, and degradation of inorganic substances, polymerization, solidification, crystallization of polymer, and so on. In addition, the pyrolysis of petroleum, the catalytic reactions of enzymes, and the thermal decomposition of coal have also been investigated.[8] Furthermore, thermal analysis kinetic methods can confirm the relationship between the thermal behavior and chemical configuration of the complexes.[9] During the course of our research,[10−20] we have prepared a series of rare earth complexes with benzoic acid or benzoic acid derivatives and nitrogen-containing ligands and reported their crystal structure, thermal decomposition mechanism, and nonisothermal kinetics. Herein, we report the synthesis, crystal structure, and thermal decomposition mechanism of a samarium complex of *p*-ClBA and 2,2′-bipyridine as coligands. Meanwhile, the kinetic parameters of the second decomposition stage were also determined jointly using a double equal−double steps method[21] and the nonlinear integral isoconversional method.[22]

* Corresponding author. Fax: +86-31186268405. Tel.: +86-31186269386. E-mail: jjzhang6@126.com.
† Experimental Center, Hebei Normal University.
‡ College of Chemistry & Material Science, Hebei Normal University.
§ Shijiazhuang Economy College.
|| Department of Chemistry, Handan College.

Experimental Section

Chemicals and Apparatus. All the reagents used were A. R. grade and were used without further purification. Sm_2O_3 (99.99 % purity) was purchased from Lanthanide Innovation Technology of Beijing Co., Ltd. $SmCl_3$ solution was prepared from Sm_2O_3 by dissolution in hydrochloric acid.

The contents of carbon, hydrogen, and nitrogen were determined by elemental analysis with a Vario-EL III element analyzer. The metal ion content was determined by EDTA titration with xylenol orange (XO) as an indicator. Infrared spectra were recorded over the frequency (4000 to 400) cm^{-1} range on a Bio-Rad FTS-135 spectrometer using KBr discs. The ultraviolet spectra were recorded on a SHIMADZU 2501 spectrophotometer in the wavelength (250 to 400) nm range. The molar conductance was determined with a Shanghai DDS-307 conductometer. The TG−DTG experiments of the title complex were obtained using a Perkin-Elmer TGA7 thermogravimetric analyzer. The heating rate was (3, 5, 7, 10, and 12) $K\cdot min^{-1}$ from room temperature to 950 °C under a static air atmosphere with the sample weight of (2.8 to 3.2) mg. A single crystal 0.24 × 0.20 × 0.18 mm in dimension was selected and mounted on a Bruker Apex II CCD diffractometer with graphite-monochromated Mo Kα radiation (λ = 0.71073 Å) at 294 K using the $\varphi-\omega$ scan technique in the range of $1.92° \le \theta \le 25.03°$. Semiempirical absorption corrections were applied using the SADABS program. The structure was solved by direct methods using the SHELXS-97 program and refined by full-matrix least-squares on F^2 using the SHELXL-97 program. All non-hydrogen atoms were refined anisotropically.

Synthesis of Complex $[Sm(p\text{-ClBA})_3bipy\cdot H_2O]_2$. The mixed ligands of *p*-HClBA (3 mmol) and 2,2′-bipyridine (1 mmol) were dissolved in 95 % ethanol, and the resultant solution was adjusted to pH = 6 to 7 by adding 1.0 $mol\cdot L^{-1}$ NaOH solution. Then the mixture was dropped into the $SmCl_3\cdot 6H_2O$ (1 mmol)

10.1021/je9002916 CCC: $40.75
Published on Web 06/04/2009

Table 1. Crystal Data and Structure Refinement for the Title Complex

item	data
empirical formula	$C_{31}H_{22}Cl_3N_2O_7Sm$
formula weight	791.21
temperature	294(2) K
wavelength	0.71073 Å
crystal system, space group	triclinic, $P\bar{1}$
unit cell dimensions	
[Å]	a = 10.192(3) Å
	b = 10.650(3) Å
	c = 14.478(4) Å
[°]	α = 85.941(4)°
	β = 77.799(4)°
	γ = 88.202(4)°
volume [nm^3]	1.5318(8)
Z, calculated density	2, 1.715 Mg·m^{-3}
absorption coefficient [mm^{-1}]	2.229
F(000)	782
crystal size	0.24 × 0.20 × 0.18 mm
θ range for data collection [°]	1.92 to 25.03
limiting indices	$-11 \le h \le 12$
	$-12 \le k \le 12$
	$-17 \le l \le 10$
reflections collected/unique	8353/5345 [$R_{(int)}$ = 0.0161]
completeness to θ = 25.03	98.7 %
absorption correction	demiempirical from equivalents
max. and min. transmission	1.000000 and 0.649223
refinement method	full-matrix least-squares on F^2
data/restraints/parameters	5345/0/397
goodness-of-fit on F^2	1.025
rinal R indices [$I > 2\sigma(I)$]	R_1 = 0.0230, wR_2 = 0.0588
R indices (all data)	R_1 = 0.0278, wR_2 = 0.0600
largest diff. peak and hole [e·Å^{-3}]	0.550 and −0.410

solution, stirred for 8 h at room temperature, and deposited for 12 h. Subsequently, the precipitates were collected by filtration and then dried in air. By slow evaporation of the mother liquor at room temperature, colorless single crystals were obtained after four weeks. The white powdery complex [Sm(p-ClBA)$_3$-bipy·H_2O]$_2$ (2.8 g, 86 %) was obtained. (Found: C, 46.76 %; H, 2.69 %; N, 3.50 %; Sm, 19.02 %. $C_{31}H_{22}Cl_3N_2O_7Sm$ requires C, 47.06 %; H, 2.80 %; N, 3.54 %; Sm, 19.00 %). UV (DMSO) λ_{max}/nm 282, 280, 260 (ε/L·mol^{-1}·cm^{-1} 33 000, 28 000, and 2000); IR(KBr) ν_{max}(film)/cm^{-1} 3420(m,b), 2360(w), 1684(s), 1591(s, ν(CN)), 1578(s), 1549(s, ν_{as}(COO^-)), 1491(w), 1476(w), 1412(s, ν_s(COO^-)), 1094(m), 1063(w), 1014(w), 992(m), 853(m), 776(s), 757(s), 689(w), 642(w), 419(m).

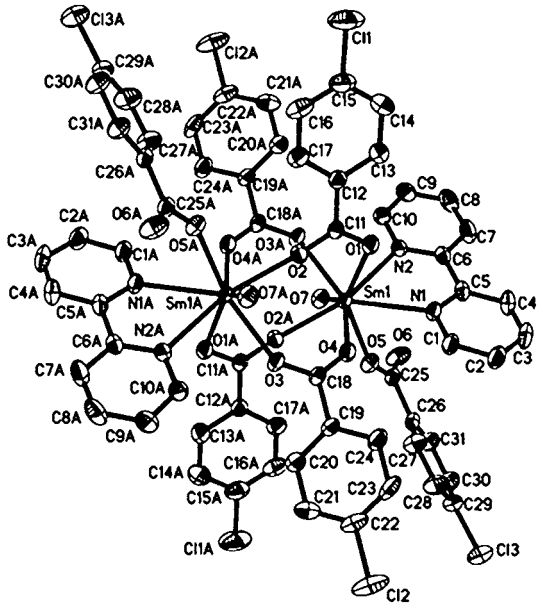

Figure 1. Molecular structure and atomic numbering of the title complex.

Methodology and Kinetic Analysis. Determination of the Function of Conversion. The equations of an iterative calculation in an accurate kinetic study[23] are as follows

$$\ln\frac{\beta}{H(x)} = \left\{\ln\left[\frac{0.0048AE}{R}\right] - \ln G(\alpha)\right\} - 1.0516\frac{E}{RT} \quad (1)$$

$$\ln\frac{\beta}{h(x)T^2} = \left[\ln\left(\frac{AR}{E}\right) - \ln G(\alpha)\right] - \frac{E}{RT} \quad (2)$$

Thereinto

$$H(x) = \frac{\exp(-x)}{0.0048\exp(-1.0516x)}h(x)$$

$$h(x) = \frac{x^4 + 18x^3 + 86x^2 + 96x}{x^4 + 20x^3 + 120x^2 + 240x + 120}$$

Equations 1 and 2 are changed into

$$\ln G(\alpha) = \ln\left(\frac{0.0048AEH(x)}{R}\right) - 1.0516\frac{E}{RT} - \ln\beta \quad (3)$$

$$\ln G(\alpha) = \ln\left(\frac{ARh(x)}{E}T^2\right) - \ln\beta \quad (4)$$

where $G(\alpha)$ is the integral mechanism function; T is the absolute temperature; A is the pre-exponential factor; R is the gas constant; E is the apparent activation energy; β is the linear heating rate; and $x = E/RT$. On substitution of the values of the conversion degrees at the same temperature on several TG curves, the different mechanism functions $G(\alpha)$,[8] and various heating rates into eq 3 or eq 4, the linear correlation coefficient r, the slope b, and the intercept a at different temperatures were obtained by a linear least-squares method with ln $G(\alpha)$ versus ln β. The relevant function is the probable mechanism function of a solid phase reaction, if the linear correlation coefficient r is the best and the slope b approaches −1.

Calculation of E and A with the Iterative Method. The activation energy calculated by plots of ln β versus $1/T$ or ln(β/T^2) versus $1/T$ based on the traditional isoconversional method is not exact, as it neglects the variation of $H(x)$ or $h(x)$ against x. However, iterative calculations considering the change can give the exact value of activation energy by plots of ln(β/H) versus $1/T$ or ln(β/hT^2) versus $1/T$, no matter how little or how great the E/RT value of the reaction is.[23]

The iterative method[28] calculated E is as follows

Step 1: Assign $H(x) = 1$ or $h(x) = 1$ to estimate the initial value of the activation energy E_1.

Step 2: Calculate $H(x)$ or $h(x)$ using E_1, then calculate a new value E_2 based on eq 1 or eq 2.

Step 3: Repeat step 2, replacing E_1 with E_2, and so on, until the absolute difference of ($E_i - E_{i-1}$) is less than a defined small quantity such as 0.1 kJ·mol^{-1}.

The last value E_i is the exact value of the activation energy of the reaction. If the reaction mechanism is known, the exact pre-exponential factor A can be calculated from the intercept of the plot at the same time.

Results and Discussion

Infrared Spectra. As seen from the IR spectra of the complex, the asymmetric vibrations ν_{as}(COO^-) at 1549 cm^{-1}, symmetric vibrations ν_s(COO^-) at 1412 cm^{-1}, and absorption band $\nu_{(Sm-O)}$

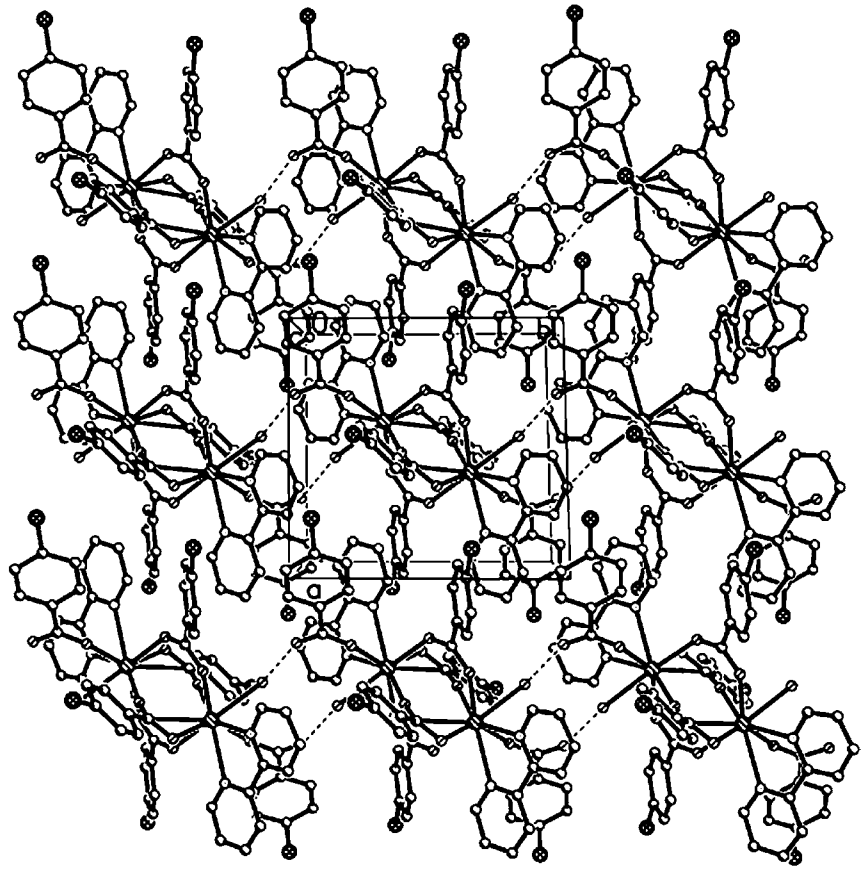

Figure 2. Crystal packing diagram of the title complex.

Table 2. Bond Lengths [Å] and Angles [°] for the Title Complex[a]

Sm(1)−O(5)	2.342(2)	Sm(1)−O(4)	2.389(2)
Sm(1)−O(2)#1	2.355(2)	Sm(1)−O(1)	2.412(2)
Sm(1)−O(3)#1	2.384(2)	Sm(1)−O(7)	2.535(2)
Sm(1)−N(2)	2.623(2)	Sm(1)−N(1)	2.633(3)
O(5)−Sm(1)−O(2)#1	84.41(8)	O(4)−Sm(1)−O(7)	140.78(8)
O(5)−Sm(1)−O(3)#1	139.61(8)	O(1)−Sm(1)−O(7)	136.90(7)
O(2)#1−Sm(1)−O(3)#1	81.95(8)	O(5)−Sm(1)−N(2)	92.44(8)
O(5)−Sm(1)−O(4)	83.32(8)	O(2)#1−Sm(1)−N(2)	148.22(8)
O(2)#1−Sm(1)−O(4)	73.20(7)	O(3)#1−Sm(1)−N(2)	80.18(7)
O(3)#1−Sm(1)−O(4)	127.68(7)	O(4)−Sm(1)−N(2)	137.96(8)
O(5)−Sm(1)−O(1)	140.92(8)	O(1)−Sm(1)−N(2)	75.61(8)
O(2)#1−Sm(1)−O(1)	124.62(7)	O(7)−Sm(1)−N(2)	72.72(8)
O(3)#1−Sm(1)−O(1)	75.76(7)	O(5)−Sm(1)−N(1)	69.24(8)
O(4)−Sm(1)−O(1)	81.72(8)	O(2)#1−Sm(1)−N(1)	143.36(8)
O(5)−Sm(1)−O(7)	69.21(8)	O(3)#1−Sm(1)−N(1)	134.50(8)
O(2)#1−Sm(1)−O(7)	76.64(7)	O(4)−Sm(1)−N(1)	78.68(8)
O(3)#1−Sm(1)−O(7)	70.68(7)	O(1)−Sm(1)−N(1)	72.50(8)
O(4)−Sm(1)−C(11)	78.76(8)	O(7)−Sm(1)−N(1)	114.45(8)
O(1)−Sm(1)−C(11)	22.63(7)	N(2)−Sm(1)−N(1)	60.99(8)
O(7)−Sm(1)−C(11)	132.86(7)	O(5)−Sm(1)−C(11)	157.64(8)
N(2)−Sm(1)−C(11)	91.98(8)	O(2)#1−Sm(1)−C(11)	102.87(8)
N(1)−Sm(1)−C(11)	94.02(8)	O(3)#1−Sm(1)−C(11)	62.75(7)

[a] #1: $-x + 1, -y + 1, -z + 1$.

Table 3. Hydrogen Bonding Data for the Title Complex[a]

D−H···A	*d*(D−H)/Å	*d*(H···A)/Å	*d*(D···A)/Å	<DHA (°)
O7−H7A···O5	0.85	2.331	2.774	112.89
O7−H7A···O6	0.85	2.394	3.132	145.50
O7−H7B···O6	0.85	1.925	2.773	175.19

[a] Symmetry codes: $-x + 1, -y + 2, -z + 1$.

at 419 cm^{-1}, are present. The strong characteristic absorption at 1684 cm^{-1} for free acid COOH disappears, indicating that the oxygen atoms of the carboxylic groups coordinate to the Sm^{3+} ion.[24] The absorption peaks of ν_{CN} (1578 cm^{-1}), δ_{C-C} (992 cm^{-1}), and δ_{C-H} (757 cm^{-1}) of the bipy ligand shift to (1591, 1014, and 776) cm^{-1} in the title complex spectrum, respectively. This can be ascribed to the blockage of respiration vibration and raising energy caused by the two nitrogen atoms coordinating to the metal ion, indicating that the nitrogen atoms of the bipy ligand coordinate to the Sm^{3+} ion.[25] The strong absorption peak at 3420 cm^{-1} in the complex confirms the presence of the water.

Ultraviolet Spectra. The complex and ligands have strong $\pi \rightarrow \pi^*$ transition absorption. The red shift of the strong absorption band at 260 nm for the free *p*-HClBA ligand to 282 nm for the complex may be explained by the π-conjugated system caused by the metal coordination.[26] Furthermore, the maximum absorption band of bipy at 280 nm is similar to that in the complex, but the molar extinction coefficient at the same wavelength is greatly enhanced, suggesting that it has even a bigger conjugated system than the free ligand, namely, forms a chelating ring.

Crystal Structure Determination. Crystal data and structural refinement, selected bond lengths, and angles and hydrogen bonding data for the complex $[Sm(p\text{-ClBA})_3bipy \cdot H_2O]_2$ are listed in Tables 1, 2, and 3, respectively. The molecular structure and atomic numbering and crystal packing diagram of the title complex and the coordination polyhedron of the Sm^{3+} ion are shown in Figures 1, 2, and 3, respectively. The title complex is a centrosymmetric binuclear molecule. The two Sm^{3+} ions are linked to each other by four carboxylic groups (O4A−C18A−O3A, O4−C18−O3, O2−C11−O1, O2A−C11A−O1A) with a bridging bidentate mode. The Sm^{3+} ion is eight-coordinated to six O and two N atoms. The six O atoms can be divided into three sets: four oxygen atoms (O1, O2A, O3A, O4) from four bridging bidentate carboxylic groups; one oxygen atom (O5) from a monodentate carboxylic group; and one coordinated water oxygen (O7). The two N atoms

Table 4. Thermal Decomposition Data for [Sm(*p*-ClBA)$_3$bipy·H$_2$O]$_2$ (β =5 K·min^{-1})

temperature range (°C)	DTG peak temperature (°C)	mass loss rate/% TG	mass loss rate/% theory	probable composition of removed groups	intermediate
59.68 to 140.63	116.05	2.09	2.28	2H$_2$O	[Sm(*p*-ClBA)$_3$bipy]$_2$
140.63 to 292.40	178.21	19.53	19.74	2bipy	[Sm(*p*-ClBA)$_3$]$_2$
292.40 to 918.25	486.07, 569.91	55.86	55.95	6*p*-ClBA-3O	Sm$_2$O$_3$
		77.84[a]	77.97[a]		

[a] Total weight loss (%).

Table 5. Conversion Degrees Measured for Given Temperatures at Different Heating Rates (Stage II)

	α				
T/K	β = 3 K·min^{-1}	β = 5 K·min^{-1}	β = 7 K·min^{-1}	β = 10 K·min^{-1}	β = 12 K·min^{-1}
453.04	0.9548	0.7712	0.6002	0.2592	0.2282
454.21	0.9579	0.8338	0.6502	0.2928	0.2645
455.14	0.9584	0.8722	0.7002	0.3284	0.2806
455.82	0.9594	0.8911	0.7502	0.3450	0.3090
456.98	0.9594	0.9259	0.8002	0.3863	0.3484

of the bipy coordinate to the Sm^{3+} ion with a chelating coordination mode to form a stable five-membered ring. In the complex, there are two lengths of the Sm−N bonds (2.623(2) to 2.633(3)) Å (mean value = 2.628 Å). The distances of the Sm−O (carboxylic groups) bonds change in the range of (2.342(2) to 2.412(2)) Å with an average distance of 2.376 Å, which is shorter than that of the Sm−N bond. Therefore, the Sm−N bond is weaker than the Sm−O bond and can be broken down prior to the Sm−O (carboxylic groups) bond. In addition, the Sm−O (coordinated water molecule) bond is more unstable and easily ruptured preceding the Sm−N bond. The above conclusions can be demonstrated by a thermal decomposition procedure.

The coordination polyhedron of the Sm^{3+} ion can be described as bicapped triangular prism geometry, where atoms N2, O1, O3A and O5, O4, O2A form lower and upper triangle planes, respectively, and the two capping atoms are the oxygen atom

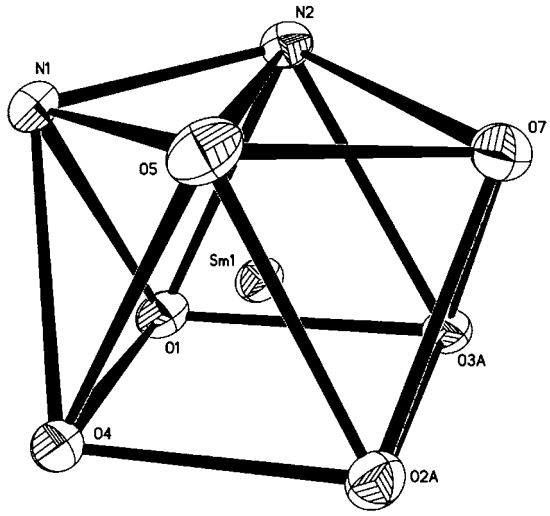

Figure 3. Coordination polydedron of the Sm^{3+}ion.

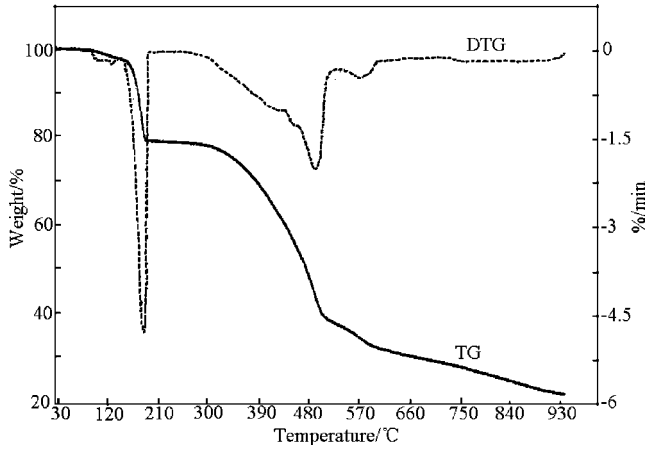

Figure 4. TG−DTG curves of the title complex at a heating rate of 5 K·min^{-1}.

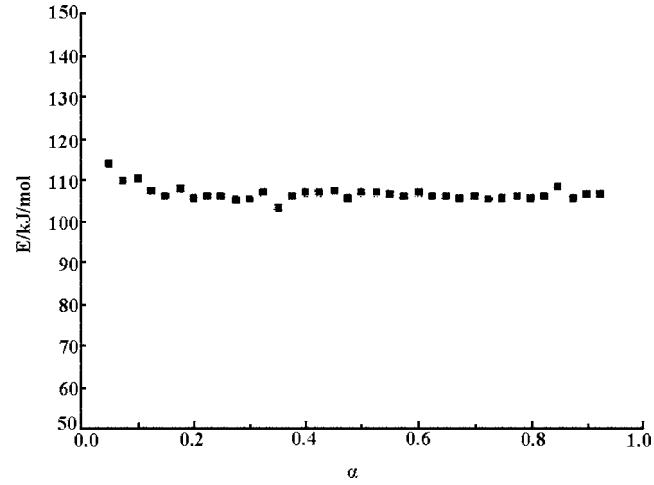

Figure 5. Relationship of *E* and α of the second decomposition stage.

Table 6. Integrant of the Results from the Linear Least Squares Method at Different Temperatures for [Sm(*p*-ClBA)$_3$bipy·H$_2$O]$_2$ (Stage II)

T/K	function no.[a]	*a*	*b*	*r*
	13	0.7202	−0.9376	−0.9858
453.04	36	2.2058	−2.0492	−0.9745
	38	**1.1029**	**−1.0246**	**−0.9745**
	13	0.7202	−0.9376	−0.9858
454.21	37	2.8668	−3.1300	−0.9952
	38	**1.1595**	**−1.0609**	**−0.9879**
	13	0.7162	−0.8716	−0.9706
455.14	37	2.9127	−3.1017	−0.9924
	38	**1.1944**	**−1.0768**	**−0.9942**
	13	0.7085	−0.8411	−0.9592
455.82	37	2.9334	−3.0561	−0.9855
	38	**1.2195**	**−1.0845**	**−0.9941**
	14	0.9301	−1.0613	−0.9422
456.98	16	0.5087	−1.0740	−0.9961
	36	2.5241	−2.1953	−0.9815
	38	**1.2621**	**−1.0976**	**−0.9815**

[a] Note: The function no. is from Tables 6 to 10 in ref 8.

Table 7. Temperatures of the Same Degree of Conversion at Different Heating Rates for the Title Complex (Stage II)

	T (K)				
α	$\beta = 3$ K·min^{-1}	$\beta = 5$ K·min^{-1}	$\beta = 7$ K·min^{-1}	$\beta = 10$ K·min^{-1}	$\beta = 12$ K·min^{-1}
0.100	427.79	433.14	436.26	444.19	445.32
0.150	431.03	436.01	439.62	448.17	449.08
0.200	433.23	438.55	441.88	450.43	451.92
0.250	435.36	440.47	443.98	452.53	454.04
0.300	436.91	442.08	445.68	454.47	455.72
0.350	438.15	443.58	447.05	456.17	457.50
0.400	439.75	444.80	448.64	457.1	458.67
0.450	440.92	446.21	449.67	458.44	459.80
0.500	442.04	447.36	450.89	459.92	460.92
0.550	443.12	448.47	451.8	461.14	462.03
0.600	444.19	449.60	453.04	462.36	463.11
0.650	445.25	450.22	454.21	463.28	464.37
0.700	446.28	451.30	455.14	464.46	465.49
0.750	446.90	452.42	455.82	465.17	466.58
0.800	447.96	453.53	456.98	466.36	467.67
0.850	450.04	454.69	458.18	467.56	469.14
0.900	450.17	456.15	459.23	468.54	470.27

(O7) of the water molecule and the N1 atom of the bipy molecule, respectively.

The oxygen (O7) of coordinated water forms two kinds of hydrogen bonds,[27] such as a tricentered hydrogen bond (O7−H7A···O5 and O7−H7A···O6) and a V model hydrogen bond (O7−H7B···O6). The oxygen (O7) forms a hydrogen bond with the oxygen atoms of the monodentate carboxylic group, rather than with the nitrogen atoms of the bipy molecule, likely due to the fact that the electronegativity of the oxygen atom is stronger than that of the nitrogen atom. The molecules are interlinked by these hydrogen bonds to form a 1-D structure, and the 1-D structure forms a 2-D supermolecular network structure along the [1, 1, 0] direction via $\pi-\pi$ stacking interactions, as shown in Figure 2. According to above-mentioned discussion, the coordination number and polyhedron of the title complex are different from those of already reported complexes, such as [Sm(*o*-ClBA)$_3$phen]$_2$ and [Eu(2,4-DClBA)$_3$-bipy]$_2$.[12,15] Furthermore, the crystal structure of the title complex is more complex due to forming a hydrogen bond.

Thermal Decomposition Process. The TG−DTG curves of the title complex obtained at a heating rate of 5 K·min^{-1} are shown in Figure 4. The thermal analytical data, the peak temperature, the temperature range of TG−DTG curves, the percentage of mass loss, and probable composition of removed groups are listed in Table 4.

As shown in the DTG curve, the thermal decomposition process of the title complex shows three states of weight loss in the measured temperature range. The first stage mass loss occurs at (59.68 to 140.63) °C with the mass loss of 2.09 % (the theoretical mass loss is 2.28 %), calculated for the loss of 2H$_2$O. The second stage occurs from (140.63 to 292.40) °C with the weight loss of 19.53 % (the theoretical mass loss is 19.74 %), which corresponds to the loss of 2bipy. The degradation can be demonstrated by the bond distance of the structure of the complex. The Sm−N (2.628 Å) distance is obviously longer than the Sm−O (carboxylic groups, 2.376 Å) bond, and theoretically, the Sm−N bond is less stable and easy to be broken down.[12] The IR spectra of the residue at 292.40 °C shows the disappearance of the absorption band of CN at 1591 cm^{-1}. The third decomposition process occurs from (292.40 to 918.25) °C with the mass loss of 55.86 %, corresponding to the loss of 6*p*-ClBA-3O. Actually, this stage is composed of two consecutive steps, and there is no obvious plateau. As seen from the IR spectra of the residue, the characteristic absorption bands of the asymmetric vibrations ν_{as}(COO$^-$) at 1549 cm^{-1} and of symmetric vibrations ν_s(COO$^-$) at 1412 cm^{-1} disappear. The characteristic absorption band of the residue is similar to the standard sample spectrum of Sm$_2$O$_3$. Therefore, by 918.25 °C, the complex [Sm(*p*-ClBA)$_3$bipy·H$_2$O]$_2$ is completely degraded into Sm$_2$O$_3$ with the total weight loss of 77.84 % (the theoretical mass loss is 77.97 %). On the basis of the above analysis, the thermal decomposition process of [Sm(*p*-ClBA)$_3$bipy·H$_2$O]$_2$ can be expressed in the following way

$$[\mathrm{Sm}(p\text{-ClBA})_3\mathrm{bipy}\cdot\mathrm{H_2O}]_2 \rightarrow [\mathrm{Sm}(p\text{-ClBA})_3\mathrm{bipy}]_2 \rightarrow [\mathrm{Sm}(p\text{-ClBA}_3)] \rightarrow \mathrm{Sm_2O_3}$$

Kinetics of the Second Decomposition Stage. The nonlinear integral isoconversional method[22] has been used to calculate the activation energy *E* of the second decomposition stage for the title complex. Figure 5 shows the relationship between *E* and α. It is clear that the values of *E* keep constant in the whole decomposition process. This fact suggests that the second decomposition stage is a single-step reaction,[28] so the probable mechanism function can be determined by means of the double equal−double steps method[21] mentioned above.

Determination of f(α) and G(α). The values of conversion degrees at different heating rates and the same temperature on the TG−DTG curves of [Sm(*p*-ClBA)$_3$bipy·H$_2$O]$_2$ are shown in Table 5. By substituting the values of α and β in Table 5 and various conversion functions into eq 3 or eq 4, using the linear least-squares method with ln $G(\alpha)$ versus ln β, the linear correlation coefficient *r*, the slope *b*, and the intercept *a* at different temperatures were obtained. The integrant results are listed in Table 6.

As shown in Table 6, one can easily see that only the coefficients *r* of the function no. 38 are the best, and the slope *b* approaches −1; hence, the probable mechanism function of the title complex is $G(\alpha) = (1-\alpha)^{(-1/2)}$, $f(\alpha) = 2(1-\alpha)^{(3/2)}$. Therefore, the second stage of the decomposition mechanism is governed by reaction chemistry.

Calculation of E and A. The values of the temperature at the same degree of conversion on five curves of the title complex are listed in Table 7.

By substituting the values of α, β, and *T* in Table 7, and the corresponding mechanism function determined above into eq 1 or eq 2, via the linear least-squares method with ln $\beta/H(x)$ versus $1/T$ or ln$(\beta/h(x)T^2)$ versus $1/T$, the activation energy *E* can be calculated from the value of the slope, and the pre-exponential factor *A* can also be calculated from the value of the intercept. The results are listed in Table 8. The values of *E* approach those calculated by the nonlinear integral isoconversional method.

Table 8. Values of the Kinetic Parameters Computed by the Iterative Method

	$\ln(\beta/H(x))$ vs $1/T$		$\ln(\beta/h(x)T^2)$ vs $1/T$	
α	$A \cdot 10^{11}$ min	E (kJ·mol^{-1})	$A \cdot 10^{11}$ min	E (kJ·mol^{-1})
0.100	72.47	110.54	71.96	110.06
0.150	18.63	106.45	18.29	105.98
0.200	13.69	105.89	13.61	105.42
0.250	14.57	106.53	14.60	106.07
0.300	10.29	105.74	10.79	105.27
0.350	5.68	103.56	5.55	103.11
0.400	15.13	107.36	15.05	106.89
0.450	16.06	107.86	16.64	107.39
0.500	13.99	107.27	13.65	106.79
0.550	12.63	106.96	12.31	106.49
0.600	13.96	107.27	13.14	106.79
0.650	11.09	106.70	11.26	106.23
0.700	10.67	106.32	10.23	105.85
0.750	9.20	105.94	9.58	105.48
0.800	10.59	106.14	10.52	105.68
0.850	23.82	108.89	23.19	108.41
0.900	15.58	106.86	15.50	106.39
average	16.94	106.84	16.82	106.37

Table 9. Thermodynamic Parameters of the Title Complex

β	$\Delta G^{\neq}$	$\Delta H^{\neq}$	$\Delta S^{\neq}$	T_P
K·min^{-1}	kJ·mol^{-1}	kJ·mol^{-1}	J·mol^{-1}·K^{-1}	K
3	112.94	102.91	−22.53	445.57
5	113.07	102.86	−22.63	451.36
7	113.14	102.83	−22.69	454.47
10	113.37	102.75	−22.87	464.59
12	113.38	102.75	−22.88	464.64
	113.18[a]	102.82[a]	−22.72[a]	456.13

[a] Average value.

The thermodynamic parameters of activation can be calculated from the equations[29,30]

$$A \exp(-E/RT) = \nu \exp(-\Delta G^{\neq}/RT) \quad (5)$$

$$\Delta H^{\neq} = E - RT \quad (6)$$

$$\Delta G^{\neq} = \Delta H^{\neq} - T\Delta S^{\neq} \quad (7)$$

where ν is the Einstein vibration frequency; $\Delta G^{\neq}$ is the Gibbs enthalpy of activation; $\Delta H^{\neq}$ is the enthalpy of activation; and $\Delta S^{\neq}$ is the entropy of activation. The values of entropy, enthalpy, and the Gibbs energy of activation at the peak temperature acquired on the basis of eqs 5 to 7 are shown in Table 9, which are changed with the temperature. By referring to Table 9, we can say that the values of $\Delta G^{\neq}$ are more than 0, indicating that the thermal decomposition process of the second step for the title complex is not spontaneous.

Conclusions

The title complex $[Sm(p\text{-ClBA})_3bipy \cdot H_2O]_2$ was synthesized, and its crystal structure was determined by single-crystal X-ray diffraction. The results showed that the Sm^{3+} ion is eight-coordinated and presents the bicapped triangular prism geometry. The thermal decomposition process of the title complex consists of three steps. The mechanism function of the second-stage thermal decomposition is $G(\alpha) = (1 - \alpha)^{(-1/2)}$, $f(\alpha) = 2(1 - \alpha)^{(3/2)}$. The activation energy E is 106.61 kJ·mol^{-1}, and the pre-exponential factor A is $16.88 \cdot 10^{11}$ min^{-1}. The enthalpy of activation $\Delta H^{\neq}$ is 102.82 kJ·mol^{-1}; the Gibbs energy of activation $\Delta G^{\neq}$ is 113.18 kJ·mol^{-1}; and the entropy of activation $\Delta S^{\neq}$ is −22.72 J·mol^{-1}·K^{-1}.

Appendix A. Supplementary Material

CCDC 642635 contains the supplementary crystallographic data for this paper. These data can be obtained free of charge via http://www.ccdc.cam.ac.uk/conts/retrieving.html, or from the Cambridge Crystallographic Data Centre, 12 Union Road, Cambridge CB2 1EZ, U.K. (fax: int.code + (1223)336−033; e-mail for inquiry: fileserv@ccdc.cam.ac.uk).

Literature Cited

(1) Wang, M.; Xu, Z. D.; Feng, D. Z. Synthesis, Spectroscopic Property and Fluorescence of Ternary Complex of Eu(III) with Nicotinic Acid and Phenanthroline. *Spectrosc. Spect. Anal.* **1999**, *19*, 484–486.

(2) Zhang, Y.; Jin, L. P.; Lü, S. Z. Crystal structure and Luminescence of $[Eu_2(BA)_6(bipy)_2]$. *Chin. J. Inorg. Chem.* **1997**, *13*, 280–287.

(3) Li, X.; Zhang, Z. Y.; Song, H. B. Sythesis, Crystal Structure and Properties of Three New Holmiums 2-fluorobenzoato Complexes. *J. Mol. Struct.* **2005**, *751*, 33–40.

(4) Jin, L. P.; Wang, R. F.; Li, L. S. Crystal structure and luminescence of europium 4-methoxybenzoate complex with 2,2′-bipyridine $[Eu(p\text{-}MOBA)_3 \cdot bipy] \cdot 1/2C_2H_5OH$. *Polyhedron* **1999**, *18*, 487–491.

(5) Li, Y.; Zheng, F. K.; Liu, X.; Zou, W. Q.; Guo, G. C.; Lu, C. Z.; Huang, J. S. Crystal Structures and Magnetic and Luminescent Properties of a Series of Homodinuclear Lanthanide Complexes with 4-Cyanobenzoic Ligand. *Inorg. Chem.* **2006**, *45*, 6308–6316.

(6) Niu, S. Y.; Jin, J.; Jin, X. L.; Yang, Z. Z. Synthesis, Strcture and Characterization of Gd(III) Dimer Bridged by Tetra Benzoates. *Solid State Sci.* **2002**, *4*, 1103–1106.

(7) Li, X.; Zhang, Z. Y.; Zou, Y. Q. Synthesis, Structure and Luminescence Properties of Four Novel Terbium2-Fluorobenzoate Complexes. *Eur. J. Inorg. Chem.* **2005**, *14*, 2909–2918.

(8) Hu, R. Z.; Gao, S. L.; Zhao, F. Q.; Shi, Q. Z.; Zhang, T. L.; Zhang, J. J. *Thermal Analysis Kinetics*, 2nd ed.; Science Press: Beijing, 2008; p *151*.

(9) Brown, M. E.; Maciezewski, M.; Vyazovkin, S.; Nomen, R.; Sempere, J.; Burnham, A.; Opfermann, J.; Strey, R.; Anderson, H. L.; Kemmler, A.; Keuleers, R.; Janssens, J.; H.; Desseyn, O.; Li, Chao-Rui.; Tang, Tong B.; Roduit, B.; Malek, J.; Mitsuhashi, T. Computational aspects of kinetic analysis: Part A: The ICTAC kinetics project-data, methods and results. *Thermochim. Acta* **2000**, *355*, 125–143.

(10) Zhang, J. J.; Ren, N.; Bai, J. H.; Xu, S. L. Synthesis and Thermal Decomposition Reaction Kinetics of Complexes of $[Sm_2(m\text{-}ClBA)_6(phen)_2] \cdot 2H_2O$ and $[Sm_2(m\text{-}BrBA)_6(phen)_2] \cdot 2H_2O$. *J. Chem. Kinet.* **2007**, *39*, 67–74.

(11) Zhang, J. J.; Ren, N.; Xu, S. L. Synthesis and Thermal Decomposition Kinetics of the Complex of Samrium p-Methybenzoate with 1,10-Phenanthroline. *Chin. J. Chem.* **2007**, *25*, 125–128.

(12) Zhang, J. J.; Ren, N.; Wang, Y. X.; Xu, S. L.; Wang, R. F.; Wang, S. P. Synthesis, Crystal Structure and Thermal Decomposition Mechanism of a Samarium o-chlorobenzoate Complex with 1,10-phenanthroline. *J. Braz. Chem. Soc.* **2006**, *17*, 1355–1359.

(13) Xu, X. L.; Zhang, J. J.; Yang, H. F.; Ren, N.; Zhang, H, Y. Synthesis, Crystal Structure and Thermal Decomposition of a Dysprosium(III) *p*-Fluorobenzoate 1,10-phenanthroline Complex. *J. Chem. Sci.* **2007**, *62b*, 51–54.

(14) Zhang, J. J.; Xu, X. L.; Ren, N.; Zhang, H. Y. Preparation, Crystal Structure and Thermal Decomposition Mechanism of Complex $[Dy(p\text{-}MOBA)_3phen]_2$. *Russ. J. Coord. Chem.* **2007**, *33*, 611–615.

(15) Tian, L.; Ren, N.; Zhang, J. J.; Liu, H. M.; Bai, J. H.; Ye, H. M.; Sun, S. J. Synthesis, Crystal structure, Luminescence and thermal decomposition kinetics of Eu(III) complex with 2,4-dichlorobenzoic acid and 2, 2′-bipyridine. *Inorg. Chim. Acta* **2009**, *362*, 3388–3394.

(16) Tian, L.; Ren, N.; Zhang, J. J.; Sun, S. J.; Ye, H. M.; Bai, J. H.; Wang, R. F. Synthesis, Crystal Structure, and Thermal Decomposition Kinetics of the Complex of Dysprosium Benzoate with 2,2′-Bipyridine. *J. Chem. Eng. Data* **2009**, *54*, 69–74.

(17) Zhang, H, Y.; Zhang, J. J.; Ren, N.; Xu, X. L.; Tian, L.; Bai, J. H. Synthesis, crystal structure and thermal decomposition mechanism of the complex $[Sm(p\text{-}BrBA)_3bipy \cdot H_2O]_2 \cdot H_2O$. *J. Alloy. Compd.* **2008**, *464*, 277–281.

(18) Zhang, H, Y.; Wu, K. Z.; Zhang, J. J.; Xu, X. L.; Ren, N.; Bai, J. H.; Tian, L. Synthesis, crystal structure and thermal decomposition kineticsof the complex $[Sm(BA)_3bipy]_2$. *Synth. Met.* **2008**, *158*, 157–164.

(19) Zhang, J. J.; Xu, X. L.; Ren, N.; Zhang, H, Y.; Tian, L. Preparation and Thermal Decomposition Reaction Kinetics of a Dysprosium(III) *p*-chlorobenzoate 1,10-phenanthroline Complex. *Int. J. Chem. Kinet.* **2008**, *40*, 66–72.

(20) Xu, X. L.; Zhang, J. J.; Ren, N.; Zhang, H, Y.; Wang, R. F.; Wang, S. P. Preparation, Structure Characterization and ThermalDecomposition Process of the Dysprosium(III) m-Methylbenzoate 1,10-Phenanthroline Complex. *S. Afr. J. Chem.* **2008**, *61*, 1–4.

(21) Zhang, J. J.; Ren, N. A New Kinetic Method of Processing TA Data. *Chin. J. Chem.* **2004**, *22*, 1459–1462.

(22) Vyazovkin, S.; Dollimore, D. Linear and Nonlinear Procedures in Isoconversional Computations of the Activation Energy of Nonisothermal Reactions in Solids. *J. Chem. Inf. Comp. Sci.* **1996**, *36*, 42–45.
(23) Gao, Z.; Nakada, M.; Amasski, I. A Consideration of Errors and Accuracy in the Isoconversional Methods. *Thermochim. Acta* **2001**, *369*, 137–142.
(24) Shi, Y. Z.; Sun, X. Z.; Jiang, Y. H. *Spectra and Chemical Identification of Organic Compounds*; Science and Technology Press: Nanjing, 1988; p 98.
(25) Wang, R. F.; Jin, L. P.; Wang, M. Z.; Huang, S. H.; Chen, X. T. Synthesis, Crystal Structure and Luminescence of Coordination Compound of Europium p-Methylbenzoate with 2,2′-Dipyridine. *Acta Chim. Sin.* **1995**, *53*, 39–45.
(26) An, B. L.; Gong, M. L.; Li, M. X.; Zhang, J. M. Synthesis, Structure and Luminescence Properties of Samarium(III) and Dysprosium(III) Complexes with a New Tridentate Organic Ligand. *J. Mol. Struct.* **2004**, *687*, 1–6.
(27) Chen, X. M.; Cai, J. W. *Single-Crystal Structure Analysis Principles and Practices*; Science press: Beijing, 2003; p 117.
(28) Lu, Z. R.; Ding, Y. C; Xu, Y.; Li, B. L.; Zhang, Y. TA Study on Four One-Dimensional Chain Copper Complexes with Benzoylacetone or 1,1,1-Trifluoro-3-(2-thenoyl)-acetone Bridged through Azobispyridine Ligands. *Chin. J. Inorg. Chem.* **2005**, *21*, 181–185.
(29) Straszko, J.; Olstak-Humienik, M.; Mozejko, J. Kinetics of Thermal Decomposition of $ZnSO_4 \cdot 7H_2O$. *Thermochim. Acta* **1997**, *292*, 145–150.
(30) Olstak-Humienik, M.; Mozejko, J. Thermodynamic Functions of Activated Complexes Created in Thermal Decomposition Processes of Sulphates. *Thermochim. Acta* **2000**, *344*, 73–79.

Received for review March 22, 2009. Accepted May 16, 2009. This project was supported by the National Natural Science Foundation of China (No.20773034), the Natural Science Foundation of Hebei Province (No.B2007000237), and the science Foundation of Hebei Normal University (No. L2006Z06).

JE9002916